

Effect of Carbon Black on the Dynamic Properties of Anisotropic Magnetorheological Elastomer

Raa Khimi Shuib^{1,2*} and Kim Louise Pickering¹

¹School of Engineering,
The University of Waikato, Hamilton,
3216, New Zealand

²School of Materials and Mineral Resources Engineering,
USM Engineering Campus, Universiti Sains Malaysia,
14300 Nibong Tebal, Pulau Pinang, Malaysia

*Corresponding author: raa_khimi@hotmail.com

Abstract: *In this work, dynamic properties of magnetorheological elastomers (MREs) based on iron sand and natural rubber; with different contents of carbon black filler (30 and 50 phr) were investigated. $\tan \delta$ was measured using dynamic mechanical analysis (DMA) over a range of frequency (0.01–130 Hz) and strain amplitude (0.1%–4.5%). $\tan \delta$ was found to be higher for anisotropic MREs with additions of carbon black, with 20%–40% improvement over the whole frequency range explored and 6%–15% improvement over the strain amplitude range explored. The results exhibited the advantages of carbon black in improving the damping performance of the MREs. The morphological characteristics of the MREs were also examined with scanning electron microscopy.*

Keywords: Magnetorheological elastomers, carbon black, damping

1. INTRODUCTION

Magnetorheological elastomers (MREs) are a new group of damping materials which consist of a non-magnetic matrix (normally an elastomer) containing a suspension of magnetically permeable particles. Damping occurs by the viscous flow of the rubber matrix and inclusion of magnetic particles in rubber enables additional damping through magnetic particle interaction and interfacial damping. Furthermore, damping and stiffness can be controlled by the application of an applied magnetic field during fabrication or in service. MREs are often referred to as the solid analogue of previously developed magnetorheological fluids (MRFs) used for example in damping of automotive suspensions. In MRFs, magnetic particles are contained within oil. The main advantage of MREs over MRFs is that particle sedimentation is overcome. Moreover, MREs do not need containers or seals to hold the fluid or prevent

leakage. MREs can be utilised for damping, either alone or within a composite structure such as those including steel plates.

MREs can be fabricated to contain a uniform suspension of magnetic particles (isotropic MREs).¹ However, it has been found that when a magnetic field is applied during curing, chain-like structures of magnetic particles are formed within the rubber (anisotropic MREs) which provides much larger damping and stiffness.^{1,2} Formation of such chain-like structures relies on the mechanism such that when individual particles are exposed to an applied magnetic field, magnetic dipole moments pointing along the field direction are induced within them. A magnetic force will cause the north pole of one particle to attract the south pole of its neighbour resulting in formation of chains and columnar structures inside the matrix. Upon curing of the matrix, the particle formation is set in place.

The magnetic particles of choice are carbonyl iron, magnetite, iron oxides, barium ferrite or Terfenol-D^{3,5} and suitable matrix materials include natural rubber, silicone rubber, polybutadiene, polyisobutylene, polyisoprene and polyurethane rubber.^{2,6-12} In this study, natural rubber was used as a matrix because of its associated ease of processing and good damping performance¹³⁻¹⁵ and iron sand was chosen as magnetic particles because it has high permeability and saturation magnetisation, low cost and is readily available in New Zealand.

The damping of MREs depends not only on the types of rubber matrix and magnetic particles, but also on the level of adhesion between the particles and the rubber matrix. Surface modification of iron sand using silane coupling agent was found to provide coupling between iron sand and natural rubber.¹⁶ It has been reported that the silane modified particles decrease the interfacial tension around the particles and results in improved dispersion of magnetic particles in isotropic MREs and an improved degree of magnetic particle alignment in anisotropic MREs.^{17,18} A number of other factors that influence the damping performance of MREs have also been reported by several authors. For instance, plasticiser has been used to soften the matrix in order to improve the degree of freedom of movement for magnetic particles during curing for anisotropic MREs and to improve the dynamic mechanical properties of isotropic and anisotropic MREs.^{14,19} It has also been reported that addition of nanosized reinforcement such as carbon black into MRE formulations can improve the damping.^{15,21}

The objective of this work is to assess the influence of carbon black on the dynamic properties of anisotropic MREs based on iron sand and natural rubber. The loss tangent, commonly called $\tan \delta$, is considered as the fundamental parameter to assess damping. $\tan \delta$ gives a comparison of the

energy lost to that stored; it is obtained by dividing the loss modulus (G'' or E'') by the storage modulus (G' or E').^{1,22}

2. EXPERIMENTAL

2.1 Materials

Natural rubber (SMR L grade) and other chemicals including zinc oxide, stearic acid, n-cyclohexyl-2-benzothiazole sulfenamide (CBS), tetramethylthiuram disulphide (TMTD), paraffin oil and naphthenic oil were all purchased from Field Rubber Limited, Auckland. Bis-(3-triethoxysilylpropyl) tetrasulphane (TESPT) was purchased from Leap LabChem Co. Limited, China. Carbon black was purchased from Shijiazhuang Changhang Co. Ltd. Iron sand was collected from Ngarunui Beach, Raglan. The iron sand was then milled using a planetary mono mill (Pulverisette 6) produced by Fristech GmbH and sieved to obtain a 45–56 μm particle size. The surface modification of iron sand was subsequently carried out using an aqueous alcohol solution method according to the procedure as described elsewhere.¹⁶

2.2 Preparation of Iron Sand and Natural Rubber MREs

The compound formulation used in this study is given in Table 1. Formulations were compounded using a conventional laboratory two roll mill (model XK150) according to ASTM designation D3184–80. The front roller speed was 24 rpm and the rear roller speed was 33 rpm, the roller diameters were 150 mm, friction ratio of two rollers was 1:1.4 and the roller temperature was set to 80°C. The nip gap (distance between front and back roller) was maintained at 2 mm during compounding. The compounding began with softening the rubber on its own in the two roll mill (mastication). Mastication reduces the viscosity and increases the plasticity of natural rubber by mean of heat generated in the two roll mill through conduction from the heated roller and shearing of rubber during milling. After 2–3 minutes the rubber became invested on the hot roll and additives (other than accelerators and sulphur) were then added followed by iron sand; addition of accelerators and sulphur were delayed to the last part of the process to prevent premature vulcanisation during compounding. The mixing time was approximately 40 minutes. The cure time at 150°C was then determined according to the procedure as described elsewhere.²³ Compounded rubber samples weighing 13 g were placed in a mould 60 × 50 × 3 mm. The anisotropic MREs were subjected to an external magnetic field at 600 mT in a specially developed electromagnetic-thermal coupled device (as shown in Figure 1) at 80°C for 30 minutes and subsequently were cured in a compression moulder at 150°C under a pressure of approximately 12 MPa. Finally, post-cure treatment

was performed by cooling the anisotropic MREs at room temperature for 30 minutes under an external magnetic field of the same strength as that used during pre-curing. The post-cure treatment was considered necessary to reorientate the magnetic dipoles after compression moulding.

Table 1: Formulation of rubber compounds.

Materials	MRE/AN	MRE/AN/30CB	MRE/AN/50CB
	(phr)	(phr)	(phr)
Natural rubber	100	100	100
ZnO	5	5	5
Stearic acid	1	1	1
Paraffin oil	2	2	2
Naphthenic oil	3	3	3
Iron sand	70	70	70
Carbon black	–	30	50
CBS	2	2	2
TMTD	1	1	1
Sulphur	1.5	1.5	1.5
Curing conditions			
Temperature (°C)	150	150	150
Pressure (MPa)	12	12	12
Magnetic field during curing (mT)	600	600	600

Notes: *phr* = per hundred rubber
MRE = Magnetorheological elastomers
ISO = Isotropic
AN = Anisotropic
CB = Carbon black
CS = Comparative sample

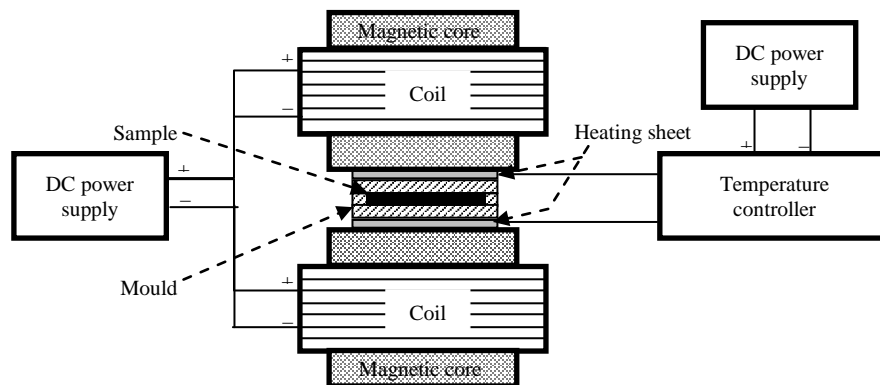


Figure 1: Sketch of specially developed electromagnetic-heat coupled device.

2.3 Dynamic Mechanical Analysis

Dynamic mechanical analysis was carried out using a Perkin Elmer dynamic mechanical analyser (DMA 8000). $\tan \delta$ was measured over a wide range of frequency and strain amplitude. The influence of frequency and strain amplitude on $\tan \delta$ was assessed using two circular disc specimens with a diameter of 10 mm and a thickness of 3 mm in shear mode at room temperature. $\tan \delta$ was measured over the frequency range of 0.01–130 Hz at fixed strain amplitude of 0.5% and over a strain amplitude range of 0.1%–4.5 % at a fixed frequency of 100 Hz.

2.4 Morphology

The microstructures of isotropic and anisotropic MREs were observed using a Hitachi S-4700 scanning electron microscope (SEM). The samples were cut into pieces with a surface area of 5×3 mm and coated with a thin layer of platinum prior to observation at an accelerating voltage of 20 kV.

3. RESULTS AND DISCUSSION

3.1 Morphology

Figure 2 shows SEM images of anisotropic MREs with and without additions of carbon black. Figure 2a shows an MRE/AN sample cured under an applied magnetic field of 600 mT at elevated temperature; as expected, the iron sand organised into chain-like columnar structures. For MRE/AN/50CB sample (Figure 2b), it can be seen that the presence of carbon black has constrained the movement of iron sand particles and the chain-like columnar structures are shorter and less aligned than MRE/AN sample.

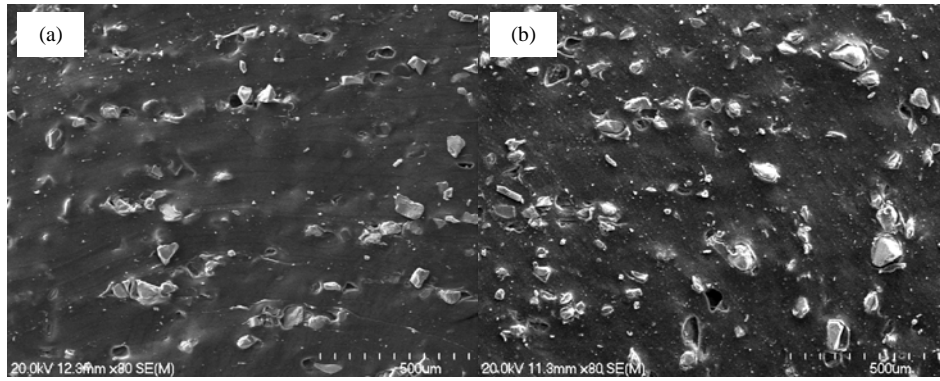


Figure 2: SEM images of surface of (a) MRE/AN and (b) MRE/AN/50CB at $\times 80$ magnitude of enlargement.

3.2 Dynamic Mechanical Analysis

3.2.1 Frequency sweep measurements

The variation of $\tan \delta$ with frequency for anisotropic MREs with different carbon black contents is depicted in Figure 3a. Generally, $\tan \delta$ increased with increasing frequency, with $\tan \delta$ values for MRE/AN found to be lower than for the others at most frequencies, although relatively larger increases in $\tan \delta$ above 100 Hz compared to other samples occurred, such that at the highest frequencies explored, $\tan \delta$ values for MRE/AN were at the upper end of those obtained. The increase of $\tan \delta$ as the frequency increased for anisotropic MREs could be due to increased energy absorbed through viscous flow of the rubber matrix and interfacial damping between the particle and the rubber matrix¹⁶ as well as potentially, energy absorbed through magnetic interactions (energy absorbed to overcome inter-particle magnetic interaction)²⁴; for samples containing carbon black, increased energy could be absorbed due to overcoming inter-particle interactions (Van der Waals).²⁵ The differences in trends observed for MREs with and without additions of carbon black are likely to be due to the relatively different amounts of energy absorbed by different mechanisms involved with different reinforcement particles at different frequencies.

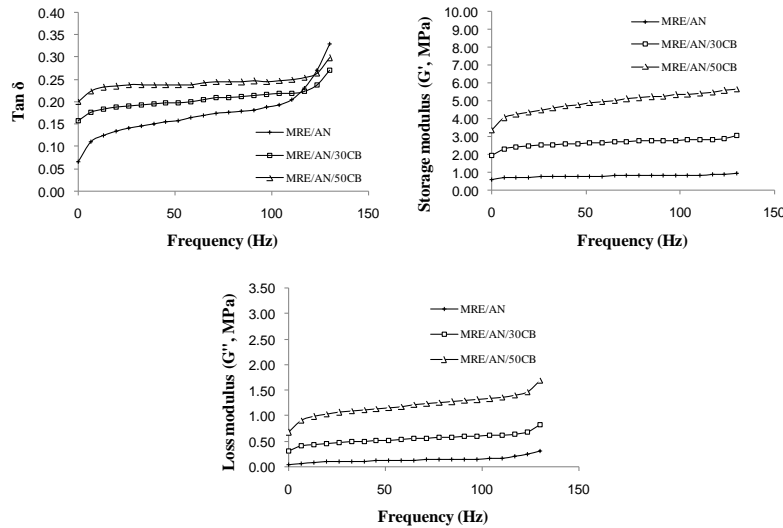


Figure 3: Tan δ , storage modulus (G') and loss modulus (G'') versus frequency for MRE/AN, MRE/AN/30CB and MRE/AN/50CB.

The results also showed that additions of carbon black gave good improvement of tan δ , the tan δ values for MRE/AN/30CB and MRE/AN/50CB were 21% and 43% higher than MRE/AN. The effect of carbon black on tan δ can be analysed further using storage modulus (G') and loss modulus (G'') plots as shown in Figure 3 (b and c). It is apparent that G' and G'' for samples containing carbon black are much higher than MRE/AN. The G' increases with increasing carbon black content up to the highest values at 50 phr carbon black. The increase in G' can be explained by increased carbon black particle-rubber interactions and carbon black particle-particle interactions as reported by number of researchers.^{25,26} The particle-rubber interactions include physical adsorption of rubber chains on carbon black filler surfaces and chemical bonding between functional groups on the surface of carbon black (mostly quinonic groups) with rubber molecular chains which will restrain the mobility of rubber on the filler surface.²⁷ The particle-particle interactions relate to the tendency of carbon black particles to form aggregates at different levels.²⁷ Carbon black aggregates agglomerate together to form what are known as primary aggregates, held together by Van der Waals bonds. Further agglomeration occurs between primary aggregates to produce secondary aggregates, again held together by Van der Waals bonds, although the secondary aggregates are less rigidly held together. The particle-rubber interactions and particle-particle interactions lead to the formation of a carbon black filler networks in the rubber matrix as shown in Figure 4. These contain rubber with different degrees of constraint (bound rubber, occluded rubber and trapped rubber), higher than that for rubber away from carbon black particles.²⁸ These constrained rubber regions improve the ability to

store elastic energy, resulting in increased G' . The increase of G'' with increasing carbon black content during deformation can be explained by the increased energy loss that occurs due to the breakdown and reformation of the carbon black filler networks.

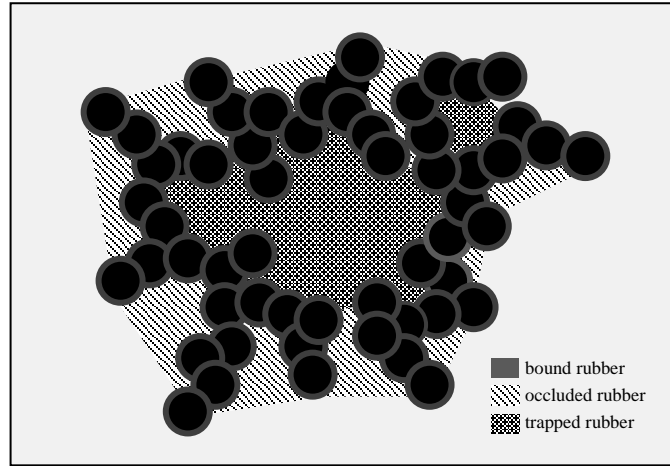


Figure 4: Schematic presentation of carbon black filler network.

3.2.2 Strain amplitude sweep measurements

The variation of $\tan \delta$ with strain amplitude for anisotropic MREs with different carbon black contents is depicted in Figure 5a. $\tan \delta$ was amplitude dependent at low strain amplitude before reaching a plateau, with increasing $\tan \delta$ for MRE/AN at around 2.5% strain amplitude, whereas for the other samples containing carbon black the $\tan \delta$ reached a plateau at around 1.5% strain amplitude. The increased amplitude dependence for MRE/AN compared to MRE/AN/30CB and MRE/AN/50CB indicates that the amplitude of applied strain required to break stronger interfacial bonding between iron sand and rubber was relatively larger compared to that required for breaking down carbon black filler networks. At the plateau region, it would appear that most of the filler-rubber interactions diminish (Van der Waals for carbon black and covalent for iron sand) and $\tan \delta$ is largely reliant on the rubber matrix which is at its largest due to greatest amount of rubber free to flow and friction between rubber chains and iron sand.^{16,29}

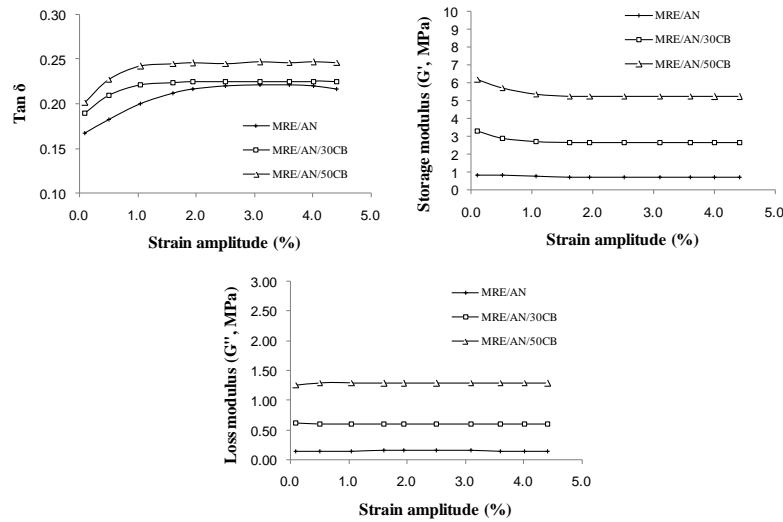


Figure 5: $\tan \delta$, storage modulus (G') and loss modulus (G'') versus strain amplitude for MRE/AN, MRE/AN/30CB and MRE/AN/50CB.

$\tan \delta$ of MRE/AN/30CB and MRE/AN/50CB were higher than MRE/AN (6% and 15%, respectively) over the whole strain amplitude range explored. Again, the effect of carbon black on improved $\tan \delta$ can be analysed further using G' and G'' plots as shown in Figure 5 (b and c). It is apparent that G' and G'' for samples containing carbon black are much higher than MRE/AN, which is not surprising given similar trends with influence of frequency on G' and G'' . As previously discussed, the increase of G' with increase in carbon black content can be explained by increased amount of constrained rubber in filler networks and the increased energy loss is likely due to breakdown and reformation of filler networks during cyclic deformation along with more constrained rubber flow.

4. CONCLUSION

It was found that alignment of magnetic particles occurred for anisotropic MREs as a consequence of curing the materials under an applied magnetic field at elevated temperature. SEM also revealed that addition of carbon black into anisotropic MREs constrained the movement of iron sand particles; chain-like columnar structures became shorter and less aligned. Energy absorption for anisotropic MREs with additions of carbon black (MRE/AN/30CB and MRE/AN/50CB) was generally found higher than MRE/AN, with 20%–40% improvement over the whole frequency range explored and 6%–15% improvement over the strain amplitude range explored. Energy absorption for

anisotropic MREs was due to viscous flow of the rubber matrix and interfacial damping between the particle and the rubber matrix as well as potentially, energy absorbed through magnetic interactions (energy absorbed to overcome inter-particle magnetic interaction). For samples containing carbon black, increased energy could be absorbed due to the breakdown and reformation of the carbon black filler networks. The results demonstrate the use of carbon black in improving the damping performance of MREs.

5. ACKNOWLEDGEMENTS

The authors would like to thank the Polymer and Composite Research Group of the University of Waikato for their support and Universiti Sains Malaysia for the scholarship.

6. REFERENCES

1. Boczkowska, A., Awietjan, S. F., Pietrzko, S. A. & Kok, J. (2012). Mechanical properties of magnetorheological elastomers under shear deformation. *Compos. Part B: Eng.*, 43(2), 636–640.
2. Chokkalingam, R., Rajasabai Senthur, P. & Mahendran, M. (2010). Magnetomechanical behavior of Fe/PU magnetorheological elastomers. *J. Compos. Mater.*, 45(15), 1545–1552.
3. Sun, Y., Zhou, X., Liu, Y., Zhao, G. & Jiang, Y. (2009). Effect of magnetic nanoparticles on the properties of magnetic rubber. *Mater. Res. Bull.*, 45(7), 878–881.
4. Makled, M. H. et al. (2005). Magnetic and dynamic mechanical properties of barium ferrite natural rubber composites. *J. Mater. Process. Tech.*, 160(2), 229–233.
5. Dobrzanski, L. A. et al. (2009). Polymer matrix composite materials reinforced by Tb_{0.3}Dy_{0.7}Fe_{1.9} magnetostrictive particles. *J. Achievements Mater. Manuf. Eng.*, 37(1), 16–23.
6. Chen, L., Gong, X. L. & Li, W. H. (2008). Effect of carbon black on the mechanical performances of magnetorheological elastomers. *Polym. Test.*, 27(3), 340–345.
7. Jerzy, K., Michal, K. & Daniel, L. (2011). Magnetomechanical properties of anisotropic and isotropic magnetorheological composites with thermoplastic elastomer matrices. *Smart Mater. Struct.*, 20(8), 12.
8. Fuchs, A. et al. (2007). Development and characterization of magnetorheological elastomers. *J. Appl. Polym. Sci.*, 105(5), 2497–2508.
9. Ginder, J. (1999). Magnetorheological elastomers: Properties and applications. *Proc SPIE.*, 3675(1), 131.

10. Lerner, A. A. & Cunefare, K. A. (2008). Performance of MRE-based Vibration absorbers. *J. Intel. Mat. Syst. Str.*, 19(5), 551–563.
11. Sun, T. L. et al. (2008). Study on the damping properties of magnetorheological elastomers based on cis-polybutadiene rubber. *Polym. Test.*, 27(4), 520–526.
12. Wang, Y. et al. (2006). Magnetorheological elastomers based on isobutylene–isoprene rubber. *Polym. Eng. Sci.*, 46(3), 264–268.
13. Blom, P. & Kari, L. (2005). Amplitude and frequency dependence of magneto-sensitive rubber in a wide frequency range. *Polym. Test.*, 24(5), 656–662.
14. Chen, L. et al. (2007). Investigation on magnetorheological elastomers based on natural rubber. *J. Mat. Sci.*, 42(14), 5483–5489.
15. Alberdi-Muniain, A., Gil-Negrete, N. & Kari, L. (2012). Influence of carbon black and plasticisers on dynamic properties of isotropic magnetosensitive natural rubber. *Plast. Rubber Compos.*, 41(7), 310–317.
16. Pickering, K. L., Raa Khimi, S. & Ilanko, S. The effect of silane coupling agent on iron sand for use in magnetorheological elastomers part 1: Surface chemical modification and characterization. *Compos. Part A: Appl. Sci. Manuf.*, 68, 377–388.
17. Xiuying, Q. et al. (2012). Microstructure and magnetorheological properties of the thermoplastic magnetorheological elastomer composites containing modified carbonyl iron particles and poly(styrene-b-ethylene-ethylenepropylene-b-styrene) matrix. *Smart Mater. Struct.*, 21(11), 115028.
18. Wang, Y. L. et al. (2006). Effects of rubber/magnetic particle interactions on the performance of magnetorheological elastomers. *Polym. Test.*, 25(2), 262–267.
19. Lokander, M. & Stenberg, B. (2003). Improving the magnetorheological effect in isotropic magnetorheological rubber materials. *Polym. Test.*, 22(6), 677–680.
20. Wu, J. et al. (2012). Improving the magnetorheological properties of polyurethane magnetorheological elastomer through plasticization. *J. Appl. Polym. Sci.*, 123(4), 2476–2484.
21. Nayak, B., Dwivedy, S. K. & Murthy, K. S. R. K. (2014). Fabrication and characterization of magnetorheological elastomer with carbon black. *J. Intel. Mater. Syst. Struct.*, 1045389(X14535011), 1–10.
22. Lakes, R. S. (2001). High Damping Composite Materials: Effect of Structural Hierarchy. *J. Compos. Mater.*, 36(3), 287–297.
23. Raa Khimi, S. & Pickering, K. L. (2013). A new method to predict optimum cure time of rubber compound using dynamic mechanical analysis. *J. Appl. Polym. Sci.*, 131(6), 1–6.

24. Kallio, M. (2005). *The elastic and damping properties of magnetorheological elastomers*. Finland: VTT Technical Research Centre of Finland.
25. Wang, M. J. (1998). Effect of polymer-filler and filler-filler interactions on dynamic properties of filled vulcanizates. *Rubber Chem. Technol.*, 71(3), 520–589.
26. Kraus, G. (1971). Reinforcement of elastomers by carbon black. In *Fortschritte der Hochpolymeren-Forschung*. Berlin: Springer Berlin Heidelberg, 155–237.
27. Jovanovic, V. et al. (2013). Composites based on carbon black reinforced NBR/EPDM rubber blends. *Compos. Part B: Eng.*, 45(1), 333–340.
28. Wang, M. J. (1999). The role of filler networking in dynamic properties of filled rubber. *Rubber Chem. Technol.*, 72(2), 430–448.
29. Rendek, M. & Lion, A. (2010). Amplitude dependence of filler-reinforced rubber: Experiments, constitutive modelling and FEM Implementation. *Int. J. Solids Struct.*, 47(21), 2918–2936.